Chin. Phys. Lett. **39**, 037801 (2022)

Nanoscale Impact Ionization and Electroluminescence in a Biased Scanning-Tunneling-Microscope Junction

Lehua Gu(顾乐华)[1], Shuang Wu(吴双)[1], Shuai Zhang(张帅)[1], and Shiwei Wu(吴施伟)[1,2,3,4*]

[1]*State Key Laboratory of Surface Physics, Key Laboratory of Micro and Nano Photonic Structures (MOE), and Department of Physics, Fudan University, Shanghai 200433, China*
[2]*Shanghai Qi Zhi Institute, Shanghai 200232, China*
[3]*Institute for Nanoelectronic Devices and Quantum Computing, Fudan University, Shanghai 200433, China*
[4]*Shanghai Research Center for Quantum Sciences, Shanghai 201315, China*

(Received 29 December 2021; accepted 13 February 2022; published online 1 March 2022)

Electroluminescence from a p-type GaAs(110) surface was induced by tunneling electrons in a scanning tunneling microscope under both polarities of bias voltage. The optical spectra exhibit a polarity-independent luminescence peak at 1.47 eV resulting from the exciton recombination. However, the quantum yield of photon emission at negative bias voltage is two orders of magnitude weaker than that at positive bias voltage. Moreover, the luminescence at negative bias voltage shows the linear dependence of bias voltage, distinct from the rapid rise due to resonant electron injection at positive bias. Furthermore, the threshold bias voltage for electroluminescence at negative bias is nearly twice the bandgap of GaAs, not simply satisfying the energy conservation for the creation of an electron–hole pair. Through theoretical calculation, we propose an impact ionization model to nicely explain the newly observed electroluminescence at negative bias voltage. We believe that this mechanism of impact ionization could be readily applied to other nanoscale optoelectronics including 2D semiconductors and 1D nanostructures.

DOI: 10.1088/0256-307X/39/3/037801

Tunneling electrons in a scanning tunneling microscope (STM) can be a local excitation source to generate photons from the nanoscale junction, which is often called STM-induced luminescence.[1,2] The combination of optical technique with the STM provides the spatial mapping of photon emission at atomic scale, unveiling the unprecedented correlation of local optical, electronic and optoelectronic properties. Up to date, the STM-induced luminescence has been widely observed from various materials such as metals,[3,4] semiconductors,[5−14] and single molecules.[15−23] While the luminescence often arises from the radiative decay of localized surface plasmon on metals and interorbital transition in molecules, there are different kinds of luminescence mechanisms in semiconductors. For indirect semiconductors such as silicon and silicon carbide, the observed electroluminescence was attributed to a localized plasmon emission[7,12] or inelastic transitions between sample surface states and tip states.[8] Meanwhile, the STM-induced luminescence in direct semiconductors such as CdS[6] and group Ⅲ–Ⅴ semiconducting heterostructures[5] is usually caused by electron–hole recombination.[9−11,13,14]

Among direct semiconductors, doped GaAs has been extensively studied for its high luminescence and promising applications in optoelectronic devices such as light-emitting diode, laser and photovoltaic cell. In an STM tunnel junction, strong luminescence was also observed in p-type GaAs(110) at positive sample bias by several research groups.[9−11,13,14] Interestingly, the electroluminescence was nearly absent at negative sample bias voltage. This polarity-dependent luminescence illustrates the electron injection from the tip to the conduction band at positive sample bias as an effective excitation mechanism to create electron–hole pair, followed by their radiative recombination at the energy of semiconducting bandgap.

In this work, we revisited the STM-induced luminescence from p-type GaAs(110) surface. Nanoscale electroluminescence spectra were observed not only at positive bias voltage but also at negative bias. Although the electroluminescence occurs at the same bandgap energy, the luminescence at negative bias voltage is about two orders of magnitude weaker than that at positive sample bias. We also found that the luminescence at negative bias voltage shows the linear dependence of bias voltage, distinct from the rapid rise due to resonant electron injection at positive bias. Furthermore, the threshold bias voltage for electroluminescence at negative bias is nearly twice the bandgap of GaAs, not simply satisfying the en-

*Corresponding author. Email: swwu@fudan.edu.cn
© 2022 Chinese Physical Society and IOP Publishing Ltd

ergy conservation for the creation of an electron–hole pair. Through theoretical calculation, we propose an impact ionization model to nicely explain the newly observed electroluminescence at negative bias voltage. We believe that this mechanism of impact ionization could be readily applied to other nanoscale optoelectronics including 2D semiconductors[24] and 1D nanostructures.[25]

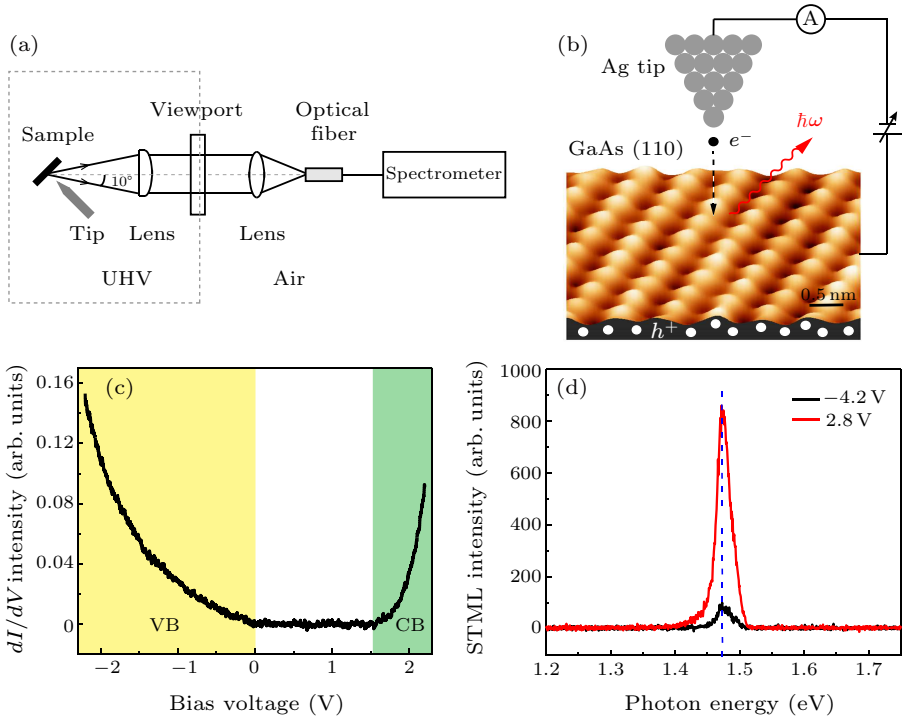

Fig. 1. STM-induced electroluminescence experimental setup and characterization of a p-type GaAs(110). (a) Schematic diagram of the experimental setup. Photons are collected by a lens in ultrahigh vacuum (UHV) and detected by a fiber-coupled spectrometer in air. (b) Schematic of STM-induced electroluminescence. The STM topographic image of cleaved p-type GaAs(110) surface was obtained with a silver tip at 16 K. Bias voltage $V_b = -3.1$ V and tunneling current $I_t = 0.1$ nA. (c) A typical dI/dV spectrum acquired on GaAs(110). The valence band (VB) and conduction band (CB) are represented by filled rectangles. The tunneling gap was set at $V_b = -2.2$ V and $I_t = 0.1$ nA. (d) Typical electroluminescence spectra measured at $V_b = 2.8$ V, $I_t = 0.1$ nA (red curve) and $V_b = -4.2$ V, $I_t = 1$ nA (black curve). The acquisition time was 60 s.

The electroluminescence experiments were carried out at 16 K by using a home-built cryogen-free low temperature STM system in ultrahigh vacuum (UHV).[26] The emitted photons from the STM junction were collected by a lens inside UHV, sent through a viewport, and detected by a fiber coupled spectrometer equipped with a CCD, as shown in Fig. 1(a). The clean GaAs(110) surface was obtained by cleaving a Zn doped p-type GaAs(100) wafer (carrier concentration $\sim 10^{19}\,\mathrm{cm}^{-3}$) in the UHV preparation chamber, and then immediately transferred to the low-temperature STM chamber for measurements. An electrochemically etched silver tip was treated on a clean Au(111) surface to optimize the efficiency of photon emission before the measurements. STM images and electroluminescence spectra were obtained in the constant current mode. The tunneling spectroscopy was conducted by using the lock-in technique with a sample bias modulation of 10 mV (rms) at 439 Hz. The bias voltage refers to sample voltage with respect to the tip.

Figure 1(b) shows a typical STM-induced luminescence process from a p-type GaAs. The tunnel junction consists of a silver tip and a p-type GaAs(110) with the majority carriers of holes. The STM topographic image of a cleaved GaAs(110) surface was obtained at $V_b = -3.1$ V. The bright protrusions represent individual As atoms since the occupied states localize at the As atoms.[27] Figure 1(c) shows a typical dI/dV spectrum that represents the local density of states on GaAs(110) surface. The position of valence band edge that lies near the Fermi level confirms the p-doping of GaAs(110). From the band edges on the dI/dV spectrum, we can extract the bandgap of about 1.55 eV.

By setting the bias voltage to either positive or negative, we observed STM-induced luminescence from the p-type GaAs(110) surface, as shown in Fig. 1(d). Both the electroluminescence spectra exhibit an emission peak at 1.47 eV with its cutoff energy of 1.51 eV, suggesting the corresponding transition from conduction band minimum to valence band

maximum [Fig. 1(c)]. We also estimated the quantum yield of the electroluminescence for both spectra. The quantum yield is 6.9×10^{-4} photons/electron at $V_b = 2.8$ V, about two orders of magnitude higher than that of 6.6×10^{-6} at $V_b = -4.2$ V. Because the STM-induced luminescence of p-type GaAs(110) at negative sample bias is very weak, this bipolar electroluminescence has not been studied previously. To acquire more information about the bipolar electroluminescence from p-type GaAs(110), we performed the detailed tunneling current- and bias voltage-dependent electroluminescence measurements.

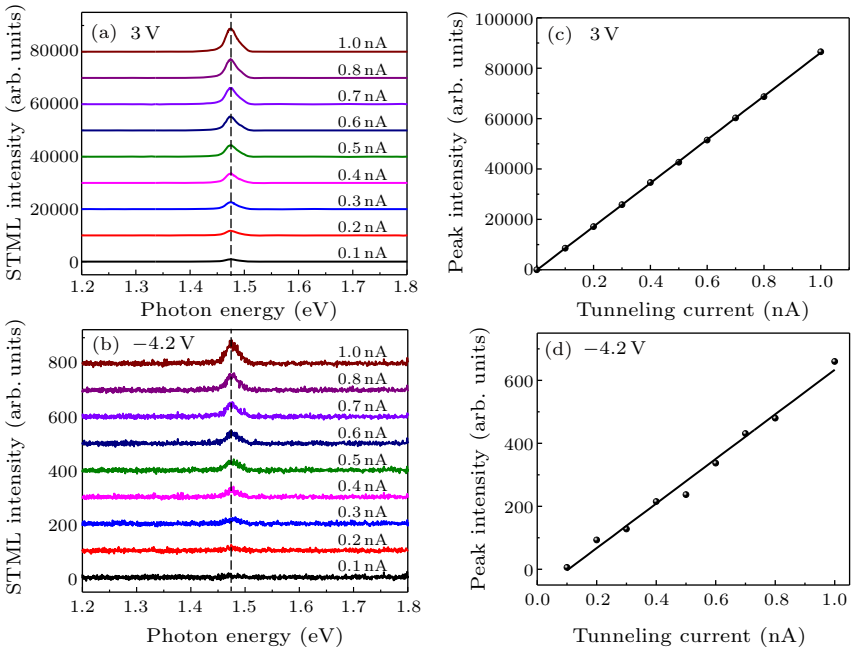

Fig. 2. Tunneling current dependence of electroluminescence spectra under both bias polarities. Electroluminescence spectra at various I_t from 0.1 to 1 nA at $V_b = 3$ V (a) and -4.2 V (b). Peak intensity of the luminescence spectra as a function of tunneling current at $V_b = 3$ V (c) and -4.2 V (d). The peak intensity was integrated from 1.472 to 1.478 eV. The vertical dashed lines denote the peak position of spectra. Solid curves are the linear fits.

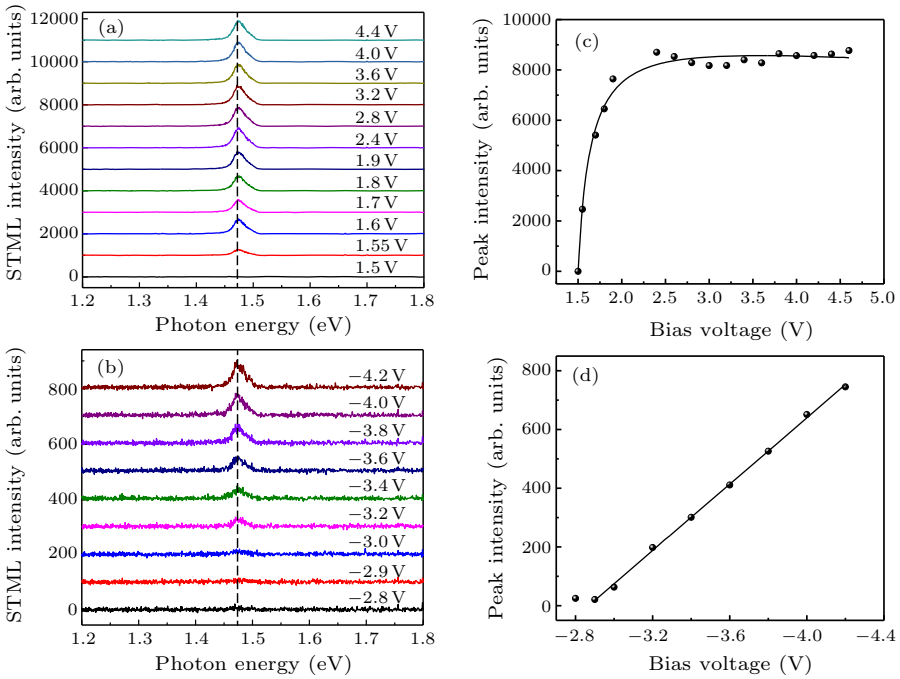

Fig. 3. Bias voltage dependence of electroluminescence spectra under both bias polarities. Electroluminescence spectra at various V_b from 1.5 to 4.4 V with $I_t = 0.1$ nA (a) and from -2.8 to -4.2 V with $I_t = 1$ nA (b). Peak intensity of luminescence spectra as a function of positive bias (c) and negative bias (d). The peak intensity was integrated from 1.472 to 1.478 eV. The vertical dashed lines denote the peak position of spectra. Solid curve in (c) is a guide to the eyes and in (d) is a linear fit.

Figures 2(a) and 2(b) show the tunneling current dependent electroluminescence spectra under positive and negative bias, respectively. The shape and peak position of spectra do not depend on the tunneling current. We extract the peak intensities and plot them with the corresponding tunneling current in Figs. 2(c) and 2(d). Both plots show the linear relationship between the luminescence intensity and tunneling current. At positive bias, the peak intensity is directly proportional to the amount of tunneling electrons which create the electron–hole pairs. However, a close examination shows an onset current of ∼0.1 nA for luminescence at negative bias voltage, indicating a different excitation mechanism for the electroluminescence in comparison to that at positive bias voltage.

The different origins of bipolar electroluminescence can be further shown by the luminescence spectra at various bias voltages. Figures 3(a) and 3(b) show the bias voltage dependent electroluminescence spectra. Again, the peak energy is independent of the bias voltage. The peak intensities as a function of bias voltage are shown in Fig. 3(c) for positive bias and Fig. 3(d) for negative bias. Clearly, the dependence of bias voltage is distinct between the positive and negative bias. At positive bias, the electroluminescence has a rapid rise starting from 1.5 V, then saturates around 2.0 V.[14] At negative bias, the threshold bias voltage appears at −2.9 V and the luminescence intensity increases almost linearly with the bias voltage. Therefore, the bias voltage dependent behaviors further suggest the different excitation mechanisms for the electroluminescence at positive and negative bias.

Figure 4 shows the schematic energy diagrams that illustrate two types of STM-induced electroluminescence processes at opposite bias voltages. Because of the electric field between the STM tip and the sample, the band bending forms at the surface of semiconducting GaAs. The direction of band bending is determined by the polarity of bias voltage. At positive bias voltage [Fig. 4(a)], when the tip Fermi level aligns with the conduction band minimum of the sample at 1.5 V, electrons from the tip have enough energy to tunnel into the sample (step 1), but have to overcome the Schottky barrier of the band bending region,[14] in addition to the vacuum barrier. The radiative recombination (step 2) between the electrons in the conduction band and holes in the valence band leads to the photon emission around 1.47 eV. Once the bias voltage is further increased, more electrons overcome the Schottky barrier and inject into the conduction band. Thus, the luminescence intensity grows rapidly and reaches a saturation at around 2 V, where the Schottky barrier is surpassed. This physical picture also explains the linear dependence of luminescence intensity on the tunneling current in Fig. 2(c).

The case is different under the negative bias voltage. At a low negative bias voltage [Fig. 4(b)], electrons can easily tunnel out of the sample because the Fermi level is close to the valence band of p-type GaAs and the tunneling process is now aided by the band bending. With the increase of negative bias voltage, some of the electrons in the valence band could lose their energy through an inelastic tunneling process (step 1) from the GaAs surface to the tip. The lost energy is used to participate in an impact ionization process (step 2), creating an electron–hole pair. The radiative recombination (step 3) of the electron–hole pair leads to the electroluminescence. If we only consider the energy conservation, the threshold bias voltage for electroluminescence would correspond to the bandgap around 1.5 eV. However, the observed threshold energy is nearly twice the bandgap of p-type GaAs.

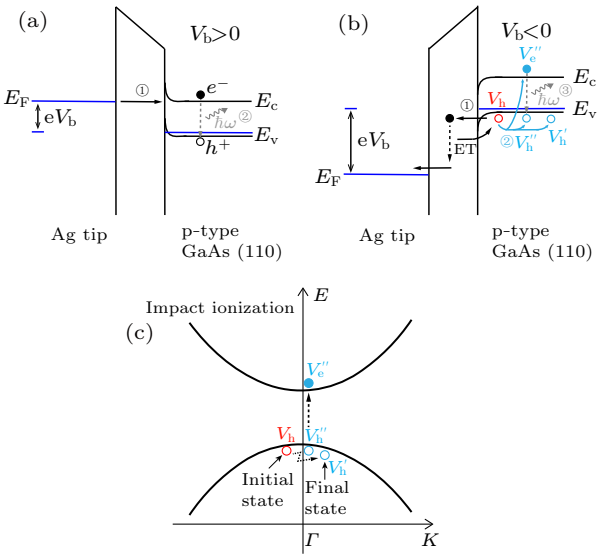

Fig. 4. Schematic energy diagrams illustrating bipolar electroluminescence processes in p-type GaAs(110). (a) Direct radiative recombination of injected electrons from the tip with holes in the valence band of p-type GaAs at positive bias voltage. (b) At negative bias voltage, some of electrons in the valence band lose their energy through an inelastic tunneling process from GaAs surface to tip. The lost energy transfers and excites electrons in valence band through an impact ionization process, as illustrated in (c). The radiative recombination of excited electron–hole pairs leads to the electroluminescence. Blue solid lines denote the Fermi level of p-type GaAs(110). ET: energy transfer. (c) The impact ionization process of energetic holes in p-type GaAs.

To resolve the contradiction, we consider an impact ionization model that has been widely used for electron multiplication in semiconductors.[28] In a reversely biased p–n junction, the electric field across the space charge layer increases with the bias voltage. Kinetic energy of carriers in space charge layer grows by accelerating in the strong electric field. When the voltage increases to a threshold, the energetic carriers can produce electron–hole pairs via impact ionization process. The threshold energy of impact ionization has to consider both the energy and momentum

conservations.[29,30] In our STM experiment, the p-type GaAs, vacuum and silver tip constitute a structure similar to p–n junctions. When a reverse bias voltage is applied to the junction (i.e. negative voltage is applied to sample), the holes in GaAs can gain energy not only from the inelastic tunneling of electrons but also by acceleration under the large electric field. Thus, the energetic holes can collide with lattice and then produce electron–hole pairs by impact ionization.

Figure 4(c) shows an initial hole locating around the valence band maximum, whose kinetic energy is gained by the electric field acceleration and determined by the applied bias voltage. After collision with lattice, it can excite a valence electron and create an electron–hole pair. In this ionization process, the phonon scattering can be neglected for simplicity because the phonon energy in GaAs is much smaller than its bandgap and threshold energy under consideration. Therefore, the ionizing hole loses energy equivalent to the sum of bandgap energy and the final kinetic energy of the created electron–hole pair. Suppose that the energy bands near the bandgap are parabolic and the impact ionization only occurs at the band edge [Fig. 4(c)], according to the conservation of energy and momentum, two equations can be obtained:

$$\frac{1}{2}m_{\rm h}v_{\rm h}^2 = E_{\rm g} + \frac{1}{2}m_{\rm h}(v_{\rm h}')^2 + \frac{1}{2}m_{\rm h}(v_{\rm h}'')^2 + \frac{1}{2}m_{\rm e}(v_{\rm e}'')^2, \tag{1}$$

$$m_{\rm h}v_{\rm h} = m_{\rm h}v_{\rm h}' + m_{\rm h}v_{\rm h}'' + m_{\rm e}v_{\rm e}'', \tag{2}$$

where $v_{\rm h}$ and $v_{\rm h}'$ are the velocities of the initial hole before and after the ionization, $v_{\rm h}''$ and $v_{\rm e}''$ are the velocities of the created hole and electron, $m_{\rm h}$ and $m_{\rm e}$ are the effective masses of the hole and electron. The minimal threshold energy for ionization can be found by taking the partial derivative of kinetic energy and momentum for the initial hole with respect to $v_{\rm h}'$, $v_{\rm h}''$ and $v_{\rm e}''$. Then we can obtain the relation

$$m_{\rm h}dv_{\rm h}''(v_{\rm h}'' - v_{\rm h}') + m_{\rm e}dv_{\rm e}''(v_{\rm e}'' - v_{\rm h}') = 0. \tag{3}$$

Since $dv_{\rm h}''$ and $dv_{\rm e}''$ are linearly independent when $m_{\rm h}v_{\rm h}$ is constant, the minimal energy occurs when the three particles have the same velocities ($v_{\rm h}' = v_{\rm h}'' = v_{\rm e}''$) after the impact ionization. The threshold energy for impact ionization is

$$E_{\rm th} = \left(\frac{1}{2}m_{\rm h}v_{\rm h}^2\right)_{\rm min} = \frac{2m_{\rm h} + m_{\rm e}}{m_{\rm h} + m_{\rm e}}E_{\rm g}, \tag{4}$$

where $m_{\rm e}$ and $m_{\rm h}$ are the effective masses for electrons and holes. For GaAs, $m_{\rm e}$ and $m_{\rm h}$ equal $0.067m_0$ and $0.38m_0$ (m_0 is the mass of a free electron), respectively.[31,32] With the bandgap of p-type GaAs ($E_{\rm g} = 1.55\,{\rm eV}$), the threshold energy $E_{\rm th}$ is estimated to be 2.87 eV, which is fairly close to the onset energy of electroluminescence at negative bias voltage [Fig. 3(d)]. Furthermore, the linear dependence of luminescence intensity on the above-threshold bias voltage can be understood with this impact ionization model.

We observed bipolar electroluminescence on a p-type GaAs(110) surface induced by tunneling electrons. The electroluminescence spectra show an emission peak at 1.47 eV when the sample bias voltage is higher than 1.5 V or lower than −2.9 V, which originates from the radiative recombination of electron–hole pairs between conduction band minimum and valence band maximum. By systematically studying the tunneling current- and bias-dependent spectra at both bias polarities, we revealed their distinct excitation mechanisms. The electron–hole pairs are generated by electron injection at positive sample bias and the impact ionization of energetic holes at negative sample bias. Furthermore, we found that the nanoscale impact ionization in a biased STM junction has to follow the principles of both energy and momentum conservations, leading to the threshold bias voltage much higher than the energy for the creation of an electron–hole pair. We believe that this new understanding could be readily applied to other nanoscale optoelectronics.[24,25] Combined with the atomic scale resolution of STM-induced electroluminescence, some novel semiconductors such as transition metal dichalcogenide monolayers[33,34] and moiré heterostructures[35] could be studied to an unprecedented level.

Acknowledgments. This work was supported by the National Key Research and Development Program of China (Grant Nos. 2019YFA0308404), the National Natural Science Foundation of China (Grant Nos. 12034003 and 91950201), the Science and Technology Commission of Shanghai Municipality (Grant No. 20JC1415900 and 2019SHZDZX01), and the Program of Shanghai Academic Research Leader (Grant No. 20XD1400300).

References

[1] Kuhnke K, Grosse C, Merino P and Kern K 2017 *Chem. Rev.* **117** 5174
[2] Schultz J F, Li S, Jiang S and Jiang N 2020 *J. Phys.: Condens. Matter* **32** 463001
[3] Berndt R, Gaisch R, Schneider W D, Gimzewski J K, Reihl B, Schlittler R R and Tschudy M 1995 *Phys. Rev. Lett.* **74** 102
[4] Uehara Y, Fujita T and Ushioda S 1999 *Phys. Rev. Lett.* **83** 2445
[5] Renaud P and Alvarado S F 1991 *Phys. Rev. B* **44** 6340
[6] Berndt R and Gimzewski J K 1992 *Phys. Rev. B* **45** 14095
[7] Downes A and Welland M E 1998 *Phys. Rev. Lett.* **81** 1857
[8] Thirstrup C, Sakurai M, Stokbro K and Aono M 1999 *Phys. Rev. Lett.* **82** 1241

[9] Yokoyama T and Takiguchi Y 2001 *Surf. Sci.* **482-485** 1163
[10] Hoshino M and Yamamoto N 2002 *MRS Online Proc. Library* **738** 723
[11] Fujita D, Onishi K and Niori N 2004 *Nanotechnology* **15** S355
[12] Baffou G, Mayne A J, Comtet G and Dujardin G 2008 *Phys. Rev. B* **77** 165320
[13] Reinhardt M, Schull G, Ebert P and Berndt R 2010 *Appl. Phys. Lett.* **96** 152107
[14] Imada H, Miwa K, Jung J, Shimizu T K, Yamamoto N and Kim Y 2015 *Nanotechnology* **26** 365402
[15] Qiu X H, Nazin G V and Ho W 2003 *Science* **299** 542
[16] Dong Z C, Guo X L, Trifonov A S, Dorozhkin P S, Miki K, Kimura K, Yokoyama S and Mashiko S 2004 *Phys. Rev. Lett.* **92** 086801
[17] Wu S W, Nazin G V and Ho W 2008 *Phys. Rev. B* **77** 205430
[18] Dong Z C, Zhang X L, Gao H Y, Luo Y, Zhang C, Chen L G, Zhang R, Tao X, Zhang Y, Yang J L and Hou J G 2010 *Nat. Photon.* **4** 50
[19] Chen C, Chu P, Bobisch C A, Mills D L and Ho W 2010 *Phys. Rev. Lett.* **105** 217402
[20] Imada H, Miwa K, Imai-Imada M, Kawahara S, Kimura K and Kim Y 2016 *Nature* **538** 364
[21] Zhang Y, Luo Y, Zhang Y, Yu Y J, Kuang Y M, Zhang L, Meng Q S, Luo Y, Yang J L, Dong Z C and Hou J G 2016 *Nature* **531** 623
[22] Doppagne B, Chong M C, Bulou H, Boeglin A, Scheurer F and Schull G 2018 *Science* **361** 251
[23] Kimura K, Miwa K, Imada H, Imai-Imada M, Kawahara S, Takeya J, Kawai M, Galperin M and Kim Y 2019 *Nature* **570** 210
[24] Miao J and Wang C 2021 *Nano Res.* **14** 1878
[25] Bulgarini G, E R M, Hocevar M, P A M B E, Kouwenhoven L P and Zwiller V 2012 *Nat. Photon.* **6** 455
[26] Zhang S, Huang D and Wu S 2016 *Rev. Sci. Instrum.* **87** 063701
[27] Feenstra R M, Stroscio J A, Tersoff J and Fein A P 1987 *Phys. Rev. Lett.* **58** 1192
[28] Sze S M and Ng K K 2006 *Physics of Semiconductor Devices* (Hoboken, NJ: Wiley)
[29] Hauser J R 1966 *J. Appl. Phys.* **37** 507
[30] Alig R C, Bloom S and Struck C W 1980 *Phys. Rev. B* **22** 5565
[31] Nakwaski W 1995 *Physica B* **210** 1
[32] Nichele F, Pal A N, Winkler R, Gerl C, Wegscheider W, Ihn T and Ensslin K 2014 *Phys. Rev. B* **89** 081306
[33] Pommier D, Bretel R, López L E P, Fabre F, Mayne A, Boer-Duchemin E, Dujardin G, Schull G, Berciaud S and Le M E 2019 *Phys. Rev. Lett.* **123** 027402
[34] Schuler B, Cochrane K A, Kastl C, Barnard E S, Wong E, Borys N J, Schwartzberg A M, Ogletree D F, Abajo F J G D and Weber-Bargioni A 2020 *Sci. Adv.* **6** eabb5988
[35] Wilson N P, Yao W, Shan J and Xu X 2021 *Nature* **599** 383